Progress In Electromagnetics Research Letters, Vol. 105, 139–147, 2022

Design and Performance Analysis of Metamaterial-Inspired Decagon-Shaped Antenna for Vehicular Communications

Subbaiyan Rajasri* and Rajasekar Boopathi Rani

Abstract—In this article, a metamaterial-inspired decagon-shaped antenna was designed with the dimensions of $30 \times 30 \times 1.6\,\text{mm}^3$ for the vehicular applications that fall under GPS (Global Positioning System), LTE (Long-Term Evolution), UMTS (Universal Mobile Telecommunication System), WLAN (Wireless Local Area Network), Wi-Fi (Wireless Fidelity), INSAT (Indian National Satellite), etc. Initially, a conventional decagon-shaped monopole antenna was designed for the frequency of 4.5 GHz. Then, a decagon-shaped metamaterial unit cell was designed for the frequencies of 1.5 GHz, 2.4 GHz, and 3.5 GHz which were inspired on the monopole antenna to obtain the desired passband characteristics under vehicular bands. All the simulations were done in the ANSYS High-Frequency Structure Simulator (HFSS) 2019 R2 version. In order to determine the metamaterial characteristics of the proposed unit cell, Scattering Parameter Retrieval Method has been used, and the values of permeability have been obtained through MATLAB. Further to examine the antenna performance in vehicular communication, it is placed on the rooftop and front side of the car model in simulation and on a physical car. Return loss characteristics were observed in the simulation as well as in the open space measurement, and the radiation pattern is analyzed with the SBR+ (Shooting and Bouncing Rays) method. The gain and radiation efficiency of the antenna get increased when it is mounted on the car model which is beneficial for the proposed application.

1. INTRODUCTION

In recent years, vehicular communication is growing rapidly due to its emerging technologies to establish Intelligent Transportation System (ITS). It provides safety precautions as well as entertainment modules. The general applications related to vehicular communications are the Global System for Mobile communication (GSM), GPS, UMTS, WLAN IEEE802.11a/b/g/n, WiMAX (Worldwide Interoperability for Microwave Access), etc. [1]. The modern vehicles are equipped with more than 20 antennas in various parts of the vehicle such as roof, spoiler, screen and windows, bumper, mirror, and trunk [2]. Many researchers are interested in reducing the number of antennas used for vehicular communication [3]. Instead of using a number of antennas for different applications, implementing an antenna with multi-operating frequencies is an essential part of the vehicular antenna research. Usually, a vehicular antenna consists of different antennas and is combined as a single module to operate at the required frequencies. By considering the compactness, instead of the module, a multiband antenna is a better solution for such cases. Many techniques have been proposed in the literature to design a multiband antenna such as slotting [4], adding stubs [5], and fractal geometries [6]. Designing a compact antenna for the vehicular application to meet the requirements such as radiation performance, gain, and impedance bandwidth altogether is a quite challenging task to antenna engineers.

Received 27 May 2022, Accepted 26 July 2022, Scheduled 3 August 2022
* Corresponding author: Subbaiyan Rajasri (rajasri2307@gmail.com).
The authors are with the Department of Electronics and Communication Engineering, National Institute of Technology, Puducherry, Karaikal-609609, India.

Metamaterial unit cell plays a vital role in designing a multiband antenna [7]. The Split Ring Resonator (SRR) of the metamaterial unit cell alters the current path and produces a new resonant frequency [8]. Usually, SRR consists of rings, and each ring creates a new resonant frequency [9]. Incorporating the SRR into the monopole antenna can create a multiband based on the required applications. In this paper, a decagon-shaped monopole antenna was designed for 4.5 GHz. To include more resonant frequencies, a decagon-shaped metamaterial unit cell was inspired on the antenna. The proposed unit cell consists of three decagon-shaped rings having split gaps alternatively. These three rings are designed for the frequencies of 1.5 GHz, 2.4 GHz, and 3.5 GHz which are more suitable for GPS, Wi-Fi/WLAN, and mobile applications. The most important advantage of the proposed antenna is its 99.79% radiation efficiency.

This paper consists of 5 sections. Besides this introductory section, Section 2 presents the design insights, construction of metamaterial-inspired multi-band antenna. Section 3 presents the parametric retrieval of the proposed metamaterial unit cell. Section 4 explains the Quasi-Static analysis of the proposed metamaterial unit cell. Section 5 presents the results and discussion of the antenna with and without car model, and finally, Section 6 provides the conclusion.

2. ANTENNA DESIGN CONSTRUCTION

Initially, a monopole antenna was proposed to achieve multibands with less design complexity, a technique called "Inspiring Metamaterial into monopole antenna" was adopted. Nowadays, metamaterial-inspired antennas are widely used for achieving compactness and multiband operations. By inspiring Split Ring Resonator (SRR) into the monopole antenna, the required band is obtained for the vehicular applications. Fig. 1(a) shows the geometry of the proposed antenna. It was designed on FR4 (Flame Retardant) material having dielectric constant 4.4 and loss tangent 0.02. The substrate material FR4 and its height as 1.6 mm were finalized based on the availability of the material. Table 1 provides the dimension details of the proposed antenna.

Table 1. Dimensions of the proposed antenna.

Variable	L_s	W_s	L_g	W_g	W_f	S
Dimension	30 mm	30 mm	8.0 mm	13 mm	3.0 mm	6.18 mm

2.1. Proposed Decagon-Shaped Monopole Antenna

The decagon-shaped monopole antenna was designed for the resonant frequency of 4.5 GHz using the formulas of circular patch antenna [10]. The radius of the circular patch with its resonant frequency 'f' is given by $a = \frac{X_{mn} \cdot c}{2\pi f \sqrt{\varepsilon_r}}$, where $X_{mn} = 1.811$ for TM_{11} mode and defined as the reactance of circular monopole antenna, and 'c' is the velocity of light in freespace. The side length of the decagon patch 'S' is calculated using $S^2 = \frac{2\pi a_e^2}{3\sqrt{3}}$ and found as $S = 6.18$ mm, where a_e is the effective radius of the patch. Fig. 1(c) shows the design flow of the proposed antenna. The highest vertical dimension of the monopole is 19 mm, and its feed is 8.5 mm. Hence, the substrate size needs to be larger than 27.5 mm. Based on the rule of thumb available in literature, the substrates lateral dimensions were finalized as 30 mm × 30 mm.

2.2. Proposed Decagon-Shaped Metamaterial Unit Cell

The proposed unit cell is analysed with the substrate dimensions of $21 \times 21 \times 1.6\,\text{mm}^3$ ($L_u \times W_u \times$ height) as shown in Fig. 1(b). Initially, the first ring of the SRR with $R_1 = 9.0$ mm, $R_2 = 8.5$ mm was inspired on the monopole antenna to achieve the resonant frequency of 1.5 GHz which is suitable for GPS application. Then the second ring was inspired on the antenna with $R_3 = 7.5$ mm, $R_4 = 6.0$ mm for the resonant frequency of 2.4 GHz which is applied to Wi-Fi and WLAN applications. Finally, the third ring was inspired on the antenna with $R_5 = 5.0$ mm, $R_6 = 4.0$ mm for the resonant frequency of

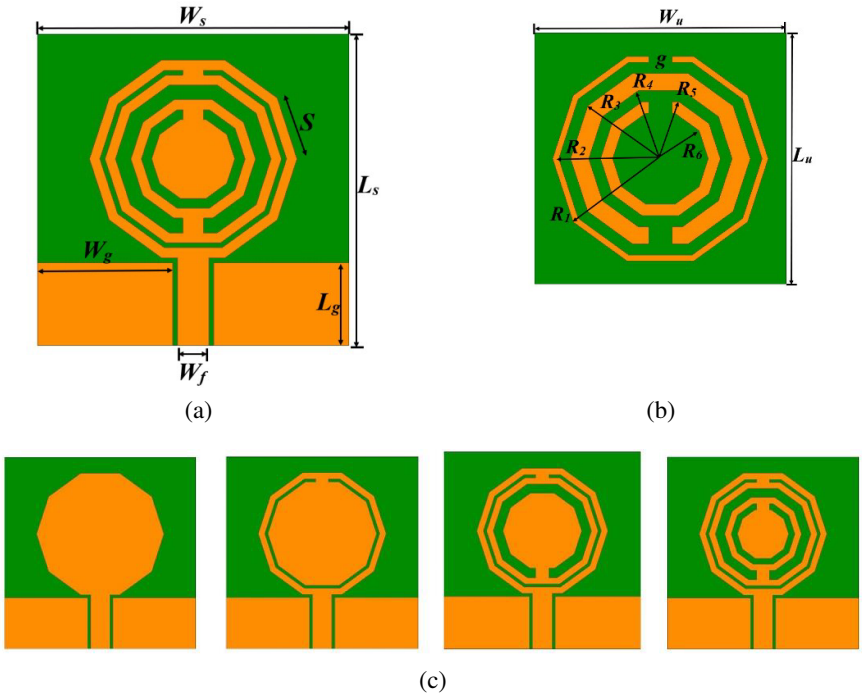

Figure 1. Geometry (a) proposed decagon-shaped metamaterial-inspired antenna, (b) proposed decagon-shaped metamaterial unit cell, (c) design flow of the proposed antenna.

3.5 GHz which is applicable to 5G mobile applications. The split gap in all the rings is $g = 2$ mm, and the gaps are positioned in alternate rings with opposite sides.

2.3. Antenna Mounted on the Rooftop of the Car

The proposed antenna is virtually placed on the rooftop of the car which is electrically larger in size than the antenna dimension as shown in Fig. 2. The antenna is also kept on the front side bumper of the car and analyzed. The simulations are performed in the ANSYS HFSS 2019 R2 version using the SBR+ method.

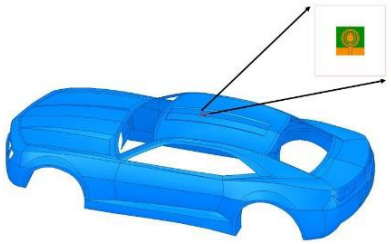

Figure 2. Antenna mounted on the rooftop of the car.

3. PARAMETER RETRIEVAL OF THE PROPOSED METAMATERIAL UNIT CELL

In order to derive the EM properties of metamaterial unit cell, it must be defined with Master-Slave boundaries on the surrounding of the waveguide. Two Floquet ports are assigned on the remaining sides of the waveguide with waves incident normally on a slab of the metamaterial to obtain the reflection (S_{11}) and transmission (S_{21}) coefficients. Fig. 3(a) shows the boundary settings for the analysis of metamaterial unit cells. If the designed SRR is inspired on the monopole antenna, the new resonant frequencies are obtained which can be validated through its effective negative values of permeability 'μ',

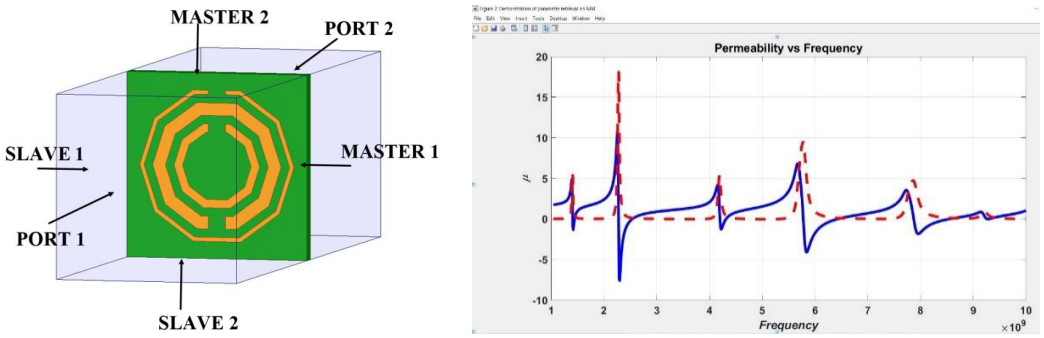

(a) (b)

Figure 3. (a) Scattering parameter retrieval method-settings, (b) permeability of the proposed metamaterial unit cell.

shown in Fig. 3(b). It is calculated using MATLAB software with the obtained results of S_{11} and S_{21} in the waveguide analysis.

4. QUASI-STATIC ANALYSIS OF THE PROPOSED METAMATERIAL UNIT CELL

The designed SRR consists of three rings with the split gap on each ring in opposite sides. Each length of the ring acts as inductances (L_1, L_2, L_3), and the space between the rings provides the capacitances (C_1, C_2, C_3). The equivalent LC tank circuit of each ring produces a new resonant frequency which is estimated by using $f_{SRR} = \frac{1}{2\pi\sqrt{L_{SRR}C_{SRR}}}$ [11]. The total length of the SRR nth ring is considered as L_n which is given as $L_n = 10[L - 2W(N-1) - 2S_a(N-1)]$, where L is the side length of the decagonal ring 'n', W the width of the ring, N the number of rings, and S_a the space between the rings. The capacitance C_{SRR} can be expressed as $C_{SRR} = (N-1)[2L - (2N-1)(W+S_a)]C_0$, where C_0 is the per-unit-length capacitance between the rings. The inductance of SRR is expressed as $L_{SRR} = 10\mu_0[l - (N-1)(S_a+W)][\ln(\frac{0.98}{\rho}) + 1.84\rho]$, in which '$\rho$' denotes the *fill ratio*.

The capacitance and inductance of the individual ring are calculated by writing MATLAB program, and the average length is chosen as the optimum side length of a particular ring. For $N = 3$, the first ring is designed with $L = 5.25$ mm, $W = 0.5$ mm, $S_a = 1$ mm for obtaining resonance at 1.5 GHz. This can be inferred with the first ring's equivalent inductance and capacitance values of 163 nH and 6.69 fF, respectively. Similarly, the second and third rings are designed for the resonant frequencies of 2.4 GHz and 3.5 GHz with the dimensions given in Section 2.2. From these, the equivalent inductance, capacitance of the second and third rings can be found as 33.1 nH, 11.5 fF and 509 nH, 42.6 fF respectively.

5. RESULTS AND DISCUSSION

5.1. Return Loss Characteristics for Different Configurations

Figure 4(a) shows the return loss characteristics of design flow for the proposed antenna, and Figure 4(b) shows the simulated and measured results of the antenna. Configuration-A resonates at the designed frequency of 4.5 GHz with a return loss of −28.42 dB. Configuration-B provides the additional frequency of 1.6 GHz with −16.70 dB return loss. Configuration-C gives the resonant frequency of 2.5 GHz with a return loss of −20.66 dB in addition to the existing resonances. Finally, Configuration-D provides the resonant frequencies of 1.5 GHz, 2.4 GHz, 3.5 GHz, and 4.5 GHz with return loss of −36.71 dB, −22.70 dB, −16.69 dB, and −20.16 dB, respectively. The obtained resonant frequencies are almost equivalent to the designed resonant frequencies. The radiation efficiency of the antenna is 93.89%.

The proposed antenna is fabricated and tested. Fig. 5(a) shows the fabricated prototype of the proposed antenna and Fig. 5(b) shows the antenna in an anechoic chamber during radiation pattern

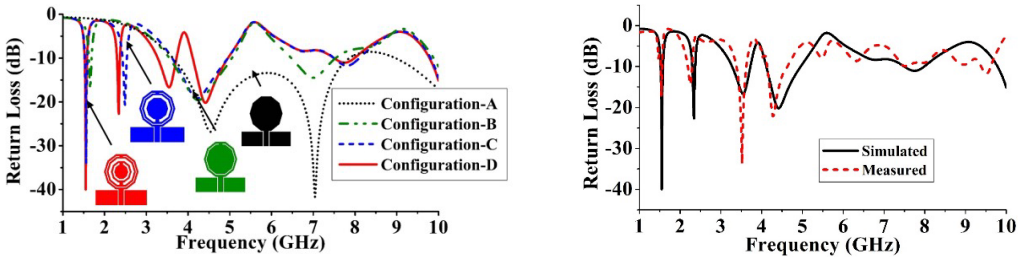

(a) (b)

Figure 4. (a) Return loss characteristics for different configurations, (b) simulated and measured return loss characteristics of the proposed antenna.

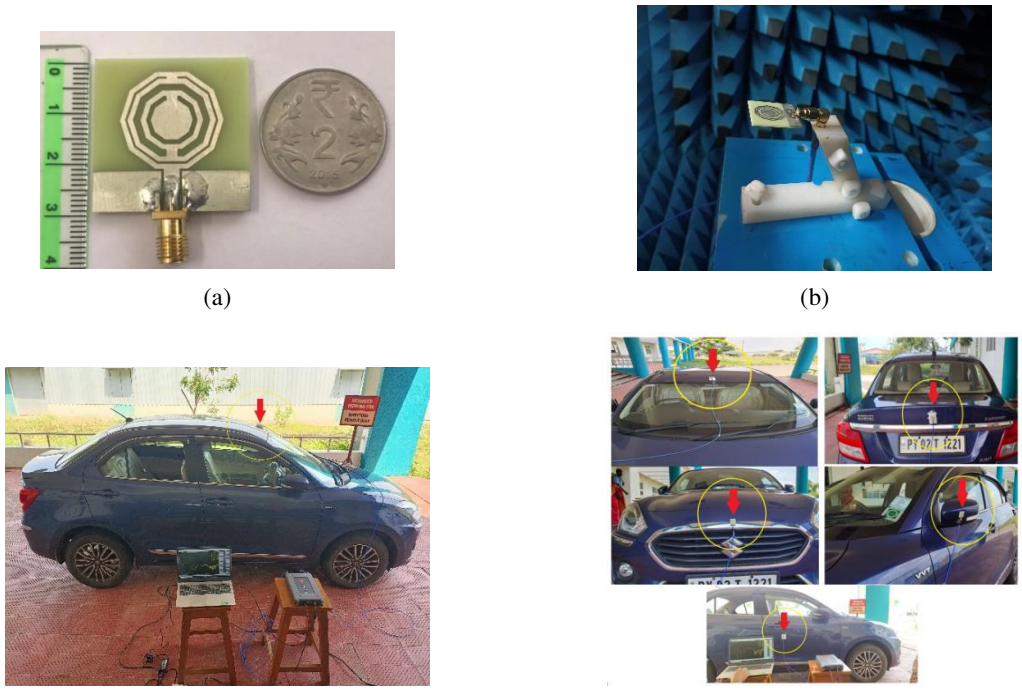

(a) (b)

(c) (d)

Figure 5. (a) Fabricated prototype of the proposed antenna, (b) proposed antenna in the anechoic chamber during radiation pattern measurement, (c) complete setup of the antenna measurement in the open environment, (d) antenna placement at different locations on car.

measurement. Fig. 5(c) shows the antenna measurement setup in the open space environment, and Fig. 5(d) shows the placement of the proposed antenna at different locations.

To check the return loss characteristics in the open environment, the proposed antenna is placed at varied places of the car such as rooftop, front bumper, back bumper, mirror, and door. In order to observe the return loss characteristics of the proposed antenna on different materials such as metal parts and plastic parts of the car, the antenna can be placed on the rooftop (metal) and front/back bumper (plastic). Here, the return loss characteristics were shown when the antenna was kept on roof top and front bumper. Figs. 6(a) and (b) show the simulated and measured return loss characteristics (S_{11}) of the antenna at the two locations. The measurement setup consists of antenna prototype, car, Keysight P9375A VNA (Vector Network Analyzer), connecting probes, and software installed laptop. Initially, the probes and connectors were calibrated, and the return loss characteristics were observed.

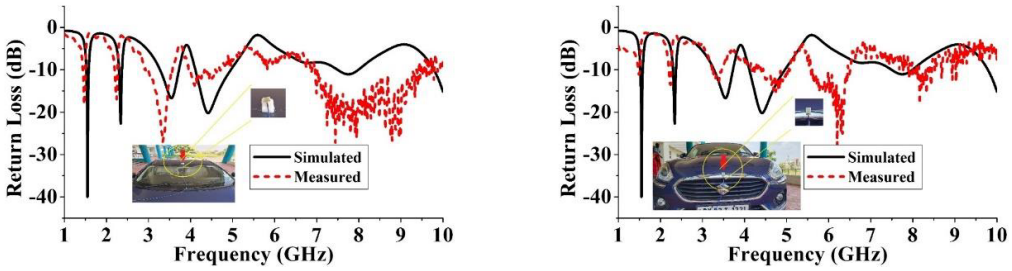

Figure 6. (a) Antenna measurement results (S_{11}) on the rooftop of the Car, (b) antenna measurement results (S_{11}) on the front bumper of the Car.

5.2. Group Delay

The group delay of the proposed antenna is shown in Fig. 7. It is measured in open environment by placing the transmitter and receiver on the rooftop of the car with a distance of 90 cm apart. The variation of group delay is found to be less than 1 ns showing good phase linearity. It clarifies that the distortion is negligible in transmission and reception of signal while using the proposed antenna.

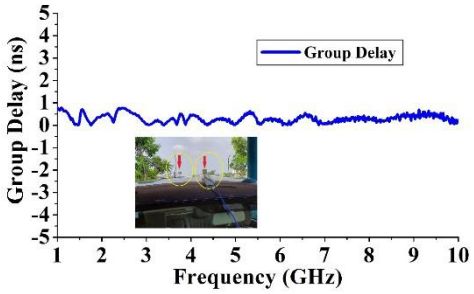

Figure 7. Group delay for the proposed antenna.

5.3. Radiation Pattern and Gain

The radiation pattern of the proposed antenna for the resonance frequencies was found using simulations and assessed with measurements. The antenna gain can be calculated using $G_{AUT} = \frac{P_{AUT}}{P_{ref}} G_{ref}$ [12], where G_{AUT} is the gain of the Antenna Under Test (AUT), P_{AUT} the power received with the AUT, P_{ref} the power received with the reference antenna, and G_{ref} the gain of the reference antenna. The gain of the proposed antenna is determined with the simulations, and the comparison is made with and without the Car model. After incorporating the antenna on the rooftop of the car model in simulation software, the radiation efficiency gets increased to 99.72%, and also the gain gets increased from 0.35 dBi, 0.44 dBi, 2.57 dBi, and 2.76 dBi to 5.91 dBi, 7.30 dBi, 8.88 dBi, and 8.60 dBi for the resonant frequencies 1.5 GHz, 2.4 GHz, 3.5 GHz, and 4.5 GHz, respectively. Fig. 8 shows the radiation pattern for different designed frequencies of the proposed antenna with and without car model. Radiation pattern of the proposed antenna is similar to the omnidirectional one. The front-to-back ratio of the radiation pattern is improved when the antenna is kept on the car. This is attributed to the increase in gain values.

Table 2 provides the comparison details of the proposed antenna with the existing antennas. The comparison uses overall dimension, substrate material, resonant frequencies, frequency bands, maximum gain, and radiation efficiency. The proposed antenna is more compact than the existing antennas; the substrate used is cost-effective; multiband is achieved; the gain obtained for the resonant frequencies is comparatively higher; and the radiation efficiency is also better. Hence, the proposed antenna will be a suitable candidate for vehicular applications.

Table 2. Comparison of the proposed work with existing work.

Ref.	Antenna Size $L \times W \times h$ (mm^3)	Substrate	Resonant frequencies (GHz)	Frequency bands (GHz)	Max. Gain (dB)	Max. Radiation efficiency (%)
[13]	139 × 124 × 7.73	LTCC, Dupont	1.83/2.18	1.77–2.22	7	90
[14]	56 × 44 × 0.8	Plexiglass	1.575/2.45/3.5/5.2	1.575–1.665/2.4–2.545/ 3.27–3.97/5.17–5.93	3.55/3.93/ 5.02/4.86	96.6
[15]	51 × 35 × 1.57	Roger's RT Duroid 5880	1.2/1.5/2.4/3.3/5.8	1.19–1.25/1.3–1.65/2.25–2.5/ 3.12–3.45/5.15–5.98	1.07/1.75/1.88/ 1.52/5.48	94.7
[16]	60 × 60 × 1.56	FR4	2.4/4.2/4.6	2.31–2.89/4.15–4.27/4.64–4.74	4.4/3.9/3.8	91
[17]	58 × 40 × 1.6	FR4	2.4/5/5.87	1.51–3.69/4.67–5.25/5.78–5.96	5.2/4.8/5	95.6
This work	30 × 30 × 1.6	FR4	1.5/2.4/3.5/4.5/7.8	1.49–1.58/2.3–2.47/3.27–3.73/ 4.11–4.96/7.48–8.00	5.91/7.30/8.88/ 8.60/8.32	99.72

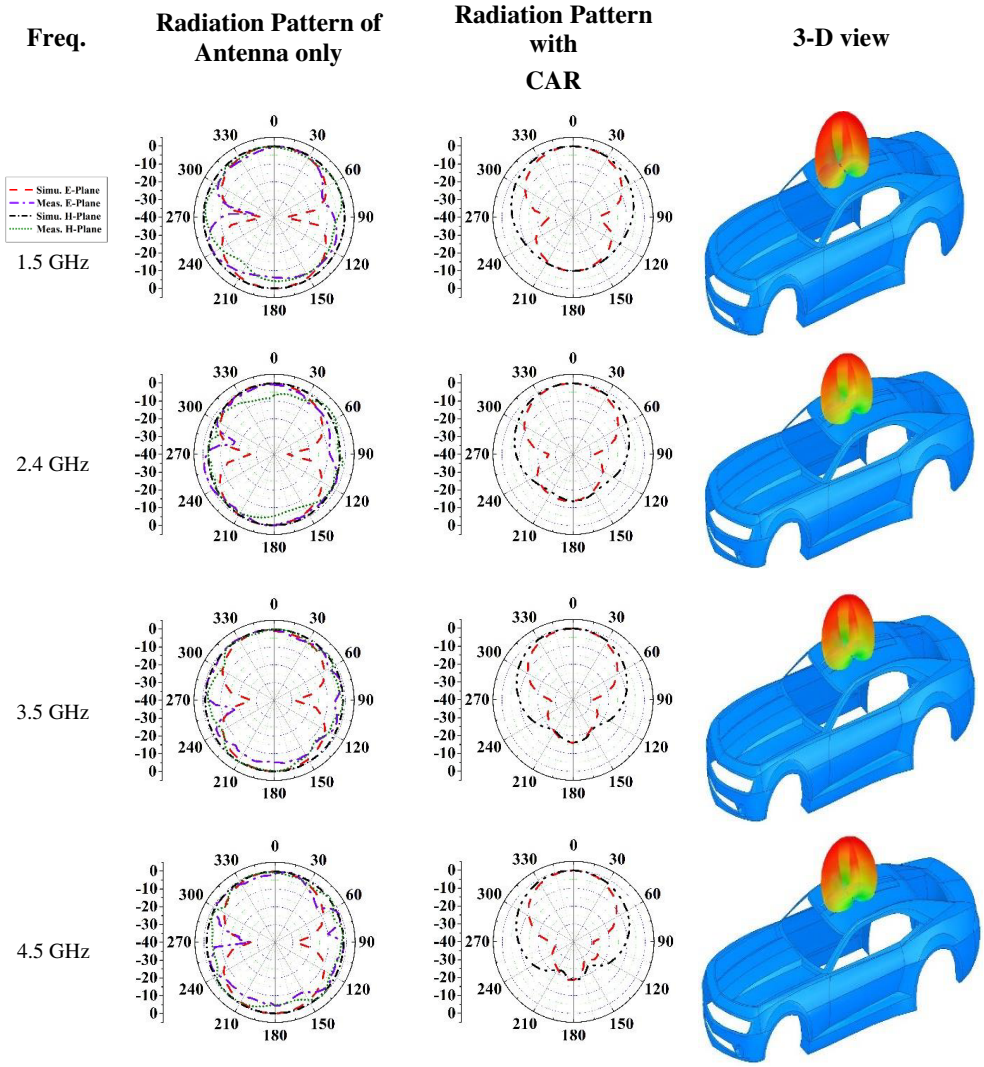

Figure 8. E-Plane and H-Plane radiation patterns.

6. CONCLUSION

This article presented the design of a metamaterial-inspired decagon-shaped antenna for vehicular applications. The proposed antenna is designed by deriving the physical dimensions analytically and then fabricated and tested. The test results reveal a good correlation between the simulated and measured values. The obtained bands are more suitable for vehicular applications such as GPS, Wi-Fi, WLAN, LTE, UMTS, and INSAT. The metamaterial properties were obtained using Scattering Parameter Retrieval Method. The performance of the antenna was analyzed in the practical environment as well as virtually by using ANSYS HFSS with the SBR+ platform. An improved antenna gain has been witnessed when the antenna is mounted on the rooftop of the vehicular body. The radiation efficiency also gets increased from 93.89% to 99.72%. Hence, the proposed antenna will spot its signature in vehicular applications.

REFERENCES

1. Madhav, B. T., T. Anilkumar, and S. K. Kotamraju, "Transparent and conformal wheel-shaped fractal antenna for vehicular communication applications," *AEU-International Journal of Electronics and Communications*, Vol. 91, 1–10, Jul. 1, 2018.
2. Phan-Huy, D. T., M. Sternad, T. Svensson, W. Zirwas, B. Villeforceix, F. Karim, and S. E. El-Ayoubi, "5G on board: How many antennas do we need on connected cars?" *IEEE Globecom Workshops*, 1–7, 2016.
3. Phan-Huy, D. T., M. Sternad, and T. Svensson, "Making 5G adaptive antennas work for very fast moving vehicles" *IEEE Intelligent Transportation System Magazine*, Vol. 7, No. 2, 71–84, 2015.
4. Xie, Y., F. C. Chen, and J. F. Qian, "Design of integrated duplexing and multi-band filtering slot antennas," *IEEE Access*, Vol. 8, 126119–126126, Jul. 3, 2020.
5. Ali, T. and R. C. Biradar, "A compact multiband antenna using $\lambda/4$ rectangular stub loaded with metamaterial for IEEE 802.11 N and IEEE 802.16 E," *Microwave and Optical Technology Letters*, Vol. 59, No. 5, 1000–1006, May 2017.
6. Deka, P. and A. De, "Design of fractal antenna for multiband operation in communication and healthcare," *2021 2nd Global Conference for Advancement in Technology (GCAT)*, 1–4, IEEE, Oct. 1, 2021.
7. Boopathi Rani, R. and S. K. Pandey, "A CPW-fed circular patch antenna inspired by reduced ground plane and CSRR slot for UWB applications with notch band," *Microwave and Optical Technology Letters*, Vol. 59, No. 4, 745–749, Apr. 2017.
8. Choudhury, A. and S. Maity, "Design and fabrication of CSRR based tunable mechanically and electrically efficient band pass filter for K-band application," *AEU-International Journal of Electronics and Communications*, Vol. 72, 134–148, Feb. 1, 2017.
9. Rajasri, S. and R. Boopathi Rani, "Analysis of unit cell with and without splits for understanding metamaterial property," *Futuristic Communication and Network Technologies*, 627–635, Springer, Singapore, 2022.
10. Balanis, C. A., *Antenna Theory: Analysis and Design*, John Wiley & Sons, Dec. 28, 2015.
11. Bilotti, F., A. Toscano, and L. Vegni, "Design of spiral and multiple split-ring resonators for the realization of miniaturized metamaterial samples," *IEEE Transactions on Antennas and Propagation*, Vol. 55, No. 8, 2258–2267, Aug. 8, 2007.
12. Kraus, J. D., R. J. Marhefka, and A. S. Khan, *Antennas and Wave Propagation*, Tata McGraw-Hill Education, 2006.
13. Kim, I. K., H. Wang, S. J. Weiss, and V. V. Varadan, "Embedded wideband metaresonator antenna on a high-impedance ground plane for vehicular applications," *IEEE Transactions on Vehicular Technology*, Vol. 61, No. 4, 1665–1672, Feb. 28, 2012.
14. Cao, Y. F., S. W. Cheung, and T. I. Yuk, "A multiband slot antenna for GPS/WiMAX/WLAN systems," *IEEE Transactions on Antennas and Propagation*, Vol. 63, No. 3, 952–958, Jan. 9, 2015.

15. Rama Rao, T., "Design and performance analysis of a penta-band spiral antenna for vehicular communications," *Wireless Personal Communications*, Vol. 96, No. 3, 3421–3434, Oct. 2017.
16. Paul, P. M., K. Kandasamy, and M. S. Sharawi, "A tri-band slot antenna loaded with split ring resonators," *Microwave and Optical Technology Letters*, Vol. 59, No. 10, 2638–2643, Oct. 2017.
17. Madhav, B. T. and T. Anilkumar, "Design and study of multiband planar wheel-like fractal antenna for vehicular communication applications," *Microwave and Optical Technology Letters*, Vol. 60, No. 8, 1985–1993, Aug. 2018.